Journal of Power Sources 219 (2012) 112–119

Contents lists available at SciVerse ScienceDirect

Journal of Power Sources

journal homepage: www.elsevier.com/locate/jpowsour

Thermo-mechanical fatigue properties of a ferritic stainless steel for solid oxide fuel cell interconnect

Yung-Tang Chiu, Chih-Kuang Lin*

Department of Mechanical Engineering, National Central University, 300 Jhong-Da Rd., Jhong-Li 32001, Taiwan

HIGHLIGHTS

- A thermo-mechanical fatigue testing technique for SOFC interconnect is developed.
- A fatigue mechanism involving cyclic plasticity dominates non-hold-time TMF life.
- Non-hold-time TMF life is increased with a decrease in applied stress at 800 °C.
- A 100-h hold-time of applied stress at 800 °C significantly reduces TMF life.
- Both creep and creep–fatigue interaction contribute to the hold-time TMF damage.

ARTICLE INFO

Article history:
Received 25 April 2012
Received in revised form
12 July 2012
Accepted 13 July 2012
Available online 21 July 2012

Keywords:
Planar solid oxide fuel cell
Interconnect
Ferritic stainless steel
Thermo-mechanical fatigue
Creep–fatigue interaction

ABSTRACT

Thermo-mechanical fatigue (TMF) behavior of a newly developed ferritic stainless steel (Crofer 22 H) for planar solid oxide fuel cell (pSOFC) interconnect is investigated. TMF tests under various combinations of cyclic mechanical and thermal loadings are conducted in air at a temperature range of 25°C–800 °C. Experimental results show the number of cycles to failure for non-hold-time TMF loading is decreased with an increase in the minimum stress applied at 800 °C. There is very little effect of maximum stress applied at 25 °C on the number of cycles to failure. The non-hold-time TMF life is dominated by a fatigue mechanism involving cyclic high-temperature softening plastic deformation. A hold-time of 100 h for the minimum stress applied at 800 °C causes a significant drop of number of cycles to failure due to a synergistic action of fatigue and creep. Creep and creep–fatigue interaction mechanisms are the two primary contributors to the hold-time TMF damage. The creep damage ratio in the hold-time TMF damage is increased with a decrease in applied stress at 800 °C and an increase in number of cycles to failure.

1. Introduction

Solid oxide fuel cell (SOFC) is one of the most efficient devices for conversion of chemical energy directly into electrical power. Among the SOFCs developed, planar SOFCs (pSOFCs) have a simple structural geometry, lower fabrication cost, and higher energy efficiency in comparison with tubular ones [1]. A typical unit cell in a pSOFC stack is composed of a positive electrode-electrolyte-negative electrode (PEN) assembly plate, a supporting window frame, a porous nickel mesh, two interconnects, and gas seals. In the early stage of pSOFC development, thickness of the electrolyte in the electrolyte-supported pSOFCs is typically larger than 100 μm. Electrolytes with a thickness of 10 μm–20 μm in the anode-supported PEN design lead to a remarkable decrease in ohmic polarization as compared to the electrolyte-supported configuration [2]. Over the past years, such a progress has been achieved in reducing the electrolyte thickness, resulting in a decrease of pSOFC operating temperature to the range of 600°C–800 °C. The reduction in operating temperature makes it possible to consider metallic alloys as interconnect materials in replacement of expensive ceramic interconnects for pSOFCs. As compared to chromium-based alloys, iron-based alloys are more attractive for use as pSOFC interconnects at an operating temperature below 800 °C due to their high ductility, good workability, and low cost [2,3]. Cr-rich ferritic stainless steels are leading candidates for pSOFC interconnects among the iron-based alloys [2,4–6].

Thermal stresses in a pSOFC stack generally result from mismatch of coefficient of thermal expansion (CTE) and thermal gradient [7,8]. Significant thermal stresses in a pSOFC stack may be induced by even a small CTE mismatch between components under

* Corresponding author. Tel.: +886 3 426 7340; fax: +886 3 425 4501.
E-mail address: t330014@cc.ncu.edu.tw (C.-K. Lin).

0378-7753/$ – see front matter © 2012 Elsevier B.V. All rights reserved.
http://dx.doi.org/10.1016/j.jpowsour.2012.07.038

thermal cycling. Therefore, metallic interconnects in a pSOFC stack may be subjected to cyclic thermal stresses during operation between periodic start-up, steady operation, and shutdown stages. As the number of start-up cycles in several designs of pSOFC system is well below 100 for stationary applications [9], the effect of such cyclic loading on metallic interconnects may promote degradation of thermo-structural integrity in a pSOFC stack and should not be neglected. An engineering component under cyclic mechanical and thermal loadings could suffer a thermo-mechanical fatigue (TMF) damage. Many components in the aerospace, power, and automotive engineering sectors are frequently subjected to such a TMF damage. The TMF damage is induced by both the stresses and temperatures varying with time. A modern servo-controlled fatigue machine is usually used to characterize TMF failure [10]. The TMF technique is more complicated than the conventional isothermal or thermal fatigue one while it has an advantage of independently controlling the stress/strain and temperature cycles on a specimen under a specified condition. Temperatures up to 800 °C in interconnects are expected at the steady-state operation of a pSOFC system [11]. According to previous analyses of thermal stress in pSOFCs [7,8], greater thermal stresses are found at 25 °C as compared to those at 800 °C due to a larger temperature difference from the stress-free assembling temperature of a pSOFC stack. Such a case with the peak (valley) stress and valley (peak) temperature present at the same time is classified as an out-of-phase TMF cycle. Therefore, a comprehensive analysis of TMF for metallic interconnects is needed in design of a reliable pSOFC system.

Most of the previous studies on the metallic interconnects developed for pSOFCs were focused on electrical conductivity, corrosion resistance, oxidation resistance, thermal properties, Cr evaporation, and long-term stability [4,12–16]. However, studies on high-temperature mechanical properties are limited for the metallic interconnect of pSOFC [17–20]. High-temperature tensile and creep properties of two newly developed, commercial Cr-rich ferritic stainless steels (Crofer 22 APU and Crofer 22 H) for pSOFC interconnects have been investigated [17–20]. Ferritic stainless steels with combined additions of Nb, W, and Si have a better creep rupture strength [18–20]. Improved tensile strength and creep resistance of Nb/W added Crofer 22 H over Crofer 22 APU are attributed to a precipitation strengthening effect of fine Laves phase particles [18,20]. However, there is still lack of study on the TMF behavior of pSOFC interconnects. As part of a series of studies on the high-temperature mechanical properties of metallic interconnects and glass sealants for pSOFCs [17,18,21–24], the TMF properties of the improved Crofer 22 H ferritic steel are investigated in the present study. Out-of-phase TMF tests as well as TMF-creep interaction tests under various combinations of mechanical loadings at a cyclic temperature range between 25 °C and 800 °C are conducted to study the long-term durability of the newly developed Crofer 22 H alloy for applications in pSOFC.

2. Experimental procedures

2.1. Material and specimen

The material used in the current study is a commercially available Crofer 22 H ferritic stainless steel supplied by the vendor in the form of cold-rolled, annealed plates with a thickness of 2.5 mm. The chemical composition, given in weight percent, of this steel is listed in Table 1. From these plates, pin-loaded specimens with a gauge section of 40 mm in length and 6 mm in width were manufactured to perform TMF tests. There is no further heat treatment performed on the specimens after machining. Details of the specimen geometry are given elsewhere [17].

2.2. Out-of-phase TMF test

Two types of out-of-phase TMF test (with or without a hold time) were conducted on a commercial closed-loop servo-hydraulic testing machine equipped with a furnace. For TMF tests without hold time, they were performed under a combination of cyclic thermal and mechanical loadings. A phase angle difference of 180° between the temperature and mechanical loading waveforms was applied and the period for each cycle was 190 min, as shown in Fig. 1(a). A minimum (maximum) mechanical load was applied at the corresponding maximum (minimum) temperature. In each cycle, the heating step with decreasing mechanical load and the cooling step with increasing mechanical load were set as 30 min and 160 min, respectively. The TMF tests were conducted in air at a cyclic temperature range between 25 °C and 800 °C to simulate the temperature range of pSOFCs between shutdown and steady operation stages. The cyclic mechanical loading was applied under force control with specified yield strength ratios (YSRs) at 25 °C and 800 °C to simulate various combinations of thermal stresses generated in interconnects of a pSOFC stack. The tensile yield strength at various temperatures has been determined under a displacement rate of 2 mm min^{-1} in a previous study [18].

Apparent YSRs of 0.2, 0.3, 0.4, 0.5, and 0.6 were selected as the applied mechanical loads at the temperatures of 25 °C and 800 °C in TMF tests. In the following, (x, y) is used to represent the applied mechanical loading. x is the YSR corresponding to the peak stress applied at room temperature while y is the YSR corresponding to the valley stress applied at 800 °C. For example, a (0.2, 0.6) TMF loading represents an applied maximum stress of 81.2 MPa with a YSR of 0.2 at 25 °C and a minimum stress of 72 MPa with a YSR of 0.6 at 800 °C. Note the tensile yield strength of Crofer 22 H is of 406 MPa at 25 °C and 120 MPa at 800 °C [18]. In this regard, mechanical loads applied at room temperature are greater than those at high temperature for all combinations even for a (0.2, 0.6) TMF loading. For TMF tests with a hold time, a hold time of 100 h was additionally applied at 800 °C for selected YSRs of 0.2 and 0.3 to study the effect of constant, thermal stress at the steady operation stage of pSOFCs. The cyclic temperature range and mechanical loadings at 25 °C in the hold-time tests were similar to those without hold time. The hold time was performed immediately after the minimum mechanical loading and maximum temperature were reached at each cycle, as shown in Fig. 1(b). As shown in Fig. 1, each TMF test started at the minimum stress with a maximum temperature of 800 °C. Note that the temperature, mechanical load, and actuator displacement of testing machine were recorded.

The procedure adopted in the TMF tests of this study is somewhat different from that in Refs. [25,26]. The cyclic mechanical loading is applied under force control in replacement of strain control used in Refs. [25,26]. The TMF specimen was initially allowed to expand under zero load during initial heating from 25 °C to 800 °C. Such a specimen can be regarded as stress-free at

Table 1
Chemical composition of Crofer 22 H stainless steel tested (wt%).

Fe	C	Cr	Mn	Si	Ti	Cu	S	P	Al	La	Nb	W
Bal.	0.007	22.93	0.43	0.21	0.07	0.02	<0.002	0.014	0.02	0.08	0.51	1.94

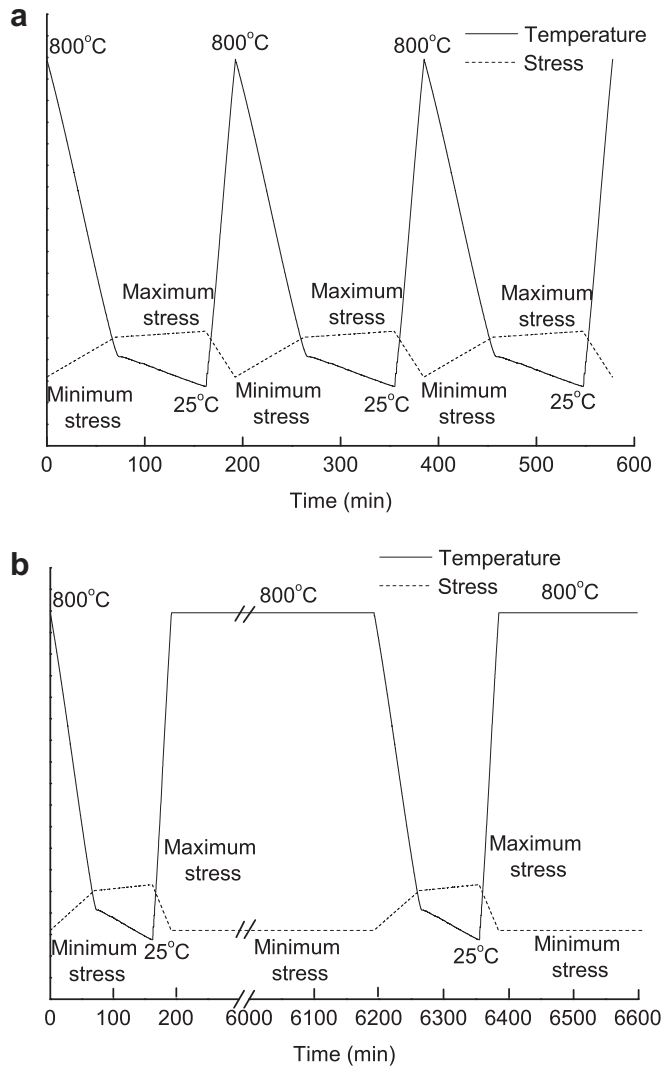

Fig. 1. Schematic of mechanical loading and temperature applied during the out-of-phase TMF test: (a) without a hold time and (b) With a hold time of 100 h.

a temperature in assembling the SOFC stack before starting the TMF test. The specified mechanical loads along with the temperature change were then applied to simulate the different levels of thermal stresses caused by CTE mismatch at 800 °C and 25 °C.

2.3. Microstructural and fractography analyses

After the TMF tests, fracture surfaces of the specimens were examined with scanning electron microscopy (SEM). In addition, some of the TMF specimens were cut axially along the loading axis, ground, and polished for metallographic preparation and observation. The microstructural change and TMF damages were then characterized and analyzed using a Hitachi SEM (Model 3500N) with secondary electrons of an accelerating voltage of 15 kV.

3. Results and discussion

3.1. Thermo-mechanical fatigue behavior without hold time

Table 2 lists the number of cycles to failure for Crofer 22 H steel subjected to various TMF loadings between 25 °C and 800 °C. Fig. 2

Table 2
Number of cycles to failure for Crofer 22 H steel under various TMF loadings between 25 °C and 800 °C.

Yield strength ratio at 25 °C	Yield strength ratio at 800 °C				
	0.2	0.3	0.4	0.5	0.6
0.2	> 102 (runout)	37	21	5	3
0.3	–	35	–	–	–
0.4	111	38	10	6	2
0.5	–	–	11	5	–
0.6	64	20	11	6	3

shows the relationship between TMF life and YSR at 800 °C for various YSRs at 25 °C. As shown in Fig. 2, the relationship between TMF life and YSR at 800 °C in a semi-log scale is well described by a linear curve for all the given YSRs at 25 °C. The number of cycles to failure is increased with a decrease in YSR at 800 °C, as shown in Fig. 2 and Table 2. The TMF life for a given YSR at 800 °C is almost independent of YSR at 25 °C. It indicates that the TMF life is dominated by the applied stress at 800 °C rather than by the applied stress at 25 °C.

Fig. 3 shows a variation of actuator displacement with time during a (0.6, 0.5) TMF test. Note that reading of the actuator displacement was reset to zero after the specified mechanical load at 800 °C was applied at beginning of each TMF test. The actuator displacement includes contributions of deformation from specimen, pin-load fixtures, and grips. However, most of it comes from the specimen deformation, particularly at high temperatures, as only the reduced section of the specimen is located within the furnace. The pin-load fixtures and grips are located outside the furnace. Therefore, the trend of actuator displacement variation can be regarded as that of specimen deformation variation. As shown in Fig. 3, specimen deformation is significantly increased with temperature in each cycle. The progressive accumulation of deformation with cycle number shown in Fig. 3 is mainly caused by a high-temperature softening effect. The cyclic plastic deformation induced by such a high-temperature softening effect apparently plays a role in the fatigue mechanism. A fatigue fracture pattern was indeed observed in Crofer 22 H specimens after a TMF test, particularly for low YSRs at 800 °C. In addition to the fatigue effect, creep deformation may occur as 72% of each TMF cycle time involves a temperature greater than 30% of the absolute melting temperature of Crofer 22 H. The melting temperature of Crofer 22 H

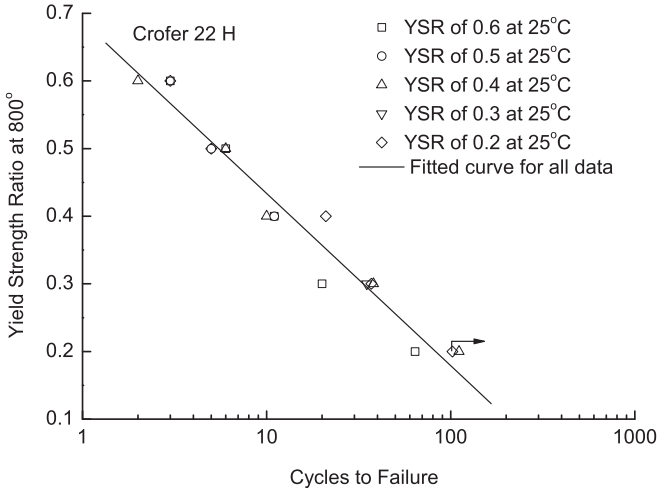

Fig. 2. Relationship between TMF life and YSR at 800 °C for Crofer 22 H steel with various YSRs at 25 °C. (Arrow designates a runout test.)

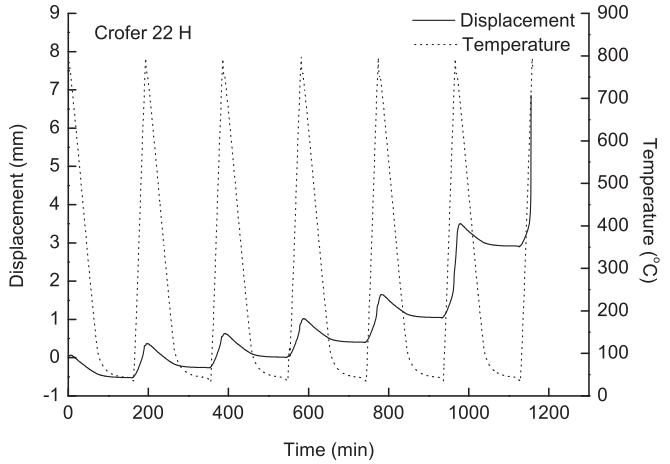

Fig. 3. Typical variation of displacement with time for Crofer 22 H steel under a (0.6, 0.5) TMF loading.

alloy is 1503 °C. Details of fractography analysis results for each corresponding damage feature are provided and discussed in a later section.

In order to characterize the contribution of a creep effect to the TMF damage, the relations between creep rupture time and applied stress for Crofer 22 H at 650°C–800 °C [18] are applied in a linear cumulative damage rule to estimate the creep damage at temperatures between 650 °C and 800 °C for each given TMF loading. The previously obtained stress–time relations for creep rupture of Crofer 22 H alloy at 650 °C, 700 °C, 750 °C, and 800 °C are given below [18]:

$$650^{o}\text{C}: \quad \sigma t_r^{0.07} = 171 \tag{1}$$

$$700^{o}\text{C}: \quad \sigma t_r^{0.08} = 126 \tag{2}$$

$$750^{o}\text{C}: \quad \sigma t_r^{0.11} = 113 \tag{3}$$

$$800^{o}\text{C}(\sigma \geqq 45\ \text{MPa}): \quad \sigma t_r^{0.13} = 82.6 \tag{4}$$

$$800^{o}\text{C}(\sigma < 45\ \text{MPa}): \quad \sigma t_r^{0.37} = 281 \tag{5}$$

where σ is the applied stress in unit of MPa, t_r is the time to rupture in unit of h. The creep rupture time for a given stress at a temperature of 650°C–800 °C is estimated by interpolating the creep rupture times given by these five equations. The creep damage ratio for each given TMF loading cycle is then obtained through a time integration of the creep damage fraction with the variation of a combined stress/temperature level at 650°C-800 °C during the TMF loading cycle. The total creep damage ratio for each given TMF test is then obtained by multiplying the number of cycles to failure by the creep damage ratio per cycle. The calculation equation of the creep damage ratio is given as follows:

$$D_c = N_f \cdot \int_0^{t_{TMF}} \frac{dt}{t_r} \tag{6}$$

where D_c is the total creep damage ratio, N_f is the number of cycles to failure, and t_{TMF} is the time interval at 650°C–800 °C for each given TMF loading cycle. Table 3 lists the total creep damage ratio for various TMF loadings. As shown in Table 3, the values of creep damage ratio for all the given TMF loadings are far less than 1. This means that the creep effect does not play an important role in determining the TMF life of a test without hold time. In this regard, the fatigue effect is the controlling mechanism for the non-hold-time TMF damages.

Table 3
Creep damage ratio for Crofer 22 H under various TMF loadings.

Yield strength ratio at 25 °C	Yield strength ratio at 800 °C				
	0.2	0.3	0.4	0.5	0.6
0.2	runout	0.0015	0.0063	0.0096	0.0259
0.3	–	0.0016	–	–	–
0.4	0.0007	0.0015	0.0032	0.0168	0.0221
0.5	–	–	0.0058	0.0174	–
0.6	0.0006	0.0010	0.0074	0.0231	0.0489

The TMF life is increased with a decrease in YSR at 800 °C, as shown in Fig. 2. Fig. 4 shows the variation of displacement with applied force for (0.6, 0.5) and (0.6, 0.2) TMF loadings. Note that the number of cycles to failure for (0.6, 0.5) and (0.6, 0.2) is 6 and 64, respectively, and only selected cycles are presented for the (0.6, 0.2) TMF loading in Fig. 4. As shown in Fig. 4, in each TMF loading cycle the displacement is increased as the maximum force (at room temperature) is decreased to the minimum force (at 800 °C). A hysteresis loop is also found for each cycle indicating an inelastic response of the given steel to the applied TMF loading. The area within the loop can be regarded as a measure of the plastic deformation work done on the specimen. Accordingly, a (0.6, 0.5) TMF loading generated a larger amount of cyclic plastic deformation than did a (0.6, 0.2) one. In addition, the cyclic force–displacement curves shift to the right (or called ratchetting) indicating an accumulation of plastic deformation in each given TMF loading. Such an accumulation of plastic deformation resulted in a failure somewhat similar to that in a tension test, when the displacement reached a certain value. The comparison of (0.6, 0.5) and (0.6, 0.2) TMF loadings given in Fig. 4 indicates that cyclic plastic deformation induced by the high-temperature softening effect is decreased when the applied mechanical loading at 800 °C was reduced from a YSR of 0.5 to 0.2. Such a reduction of cyclic plastic deformation leads to an increase in number of cycles to failure. Therefore, the increase in TMF life with decreasing YSR at 800 °C is attributed to a less amount of high-temperature softening plastic deformation.

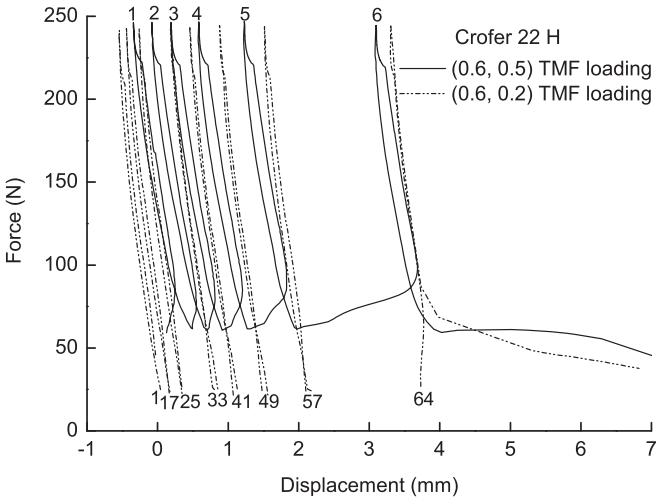

Fig. 4. Cyclic force–displacement curves for Crofer 22 H steel under (0.6, 0.5) and (0.6, 0.2) TMF loadings. (Note that cycle numbers are labeled for the corresponding hysteresis loops in each TMF test.)

3.2. Thermo-mechanical fatigue behavior with a hold time

Interconnects should exhibit adequate high-temperature mechanical strength and creep resistance. This requirement is of particular importance to a pSOFC stack since interconnects serve as a structural support during a long-term, high-temperature steady operation of a pSOFC system. Therefore, creep properties of the Crofer 22 APU and Crofer 22 H alloys for SOFC interconnects have been characterized in previous studies [17,18]. In addition to the steady operation stage, interconnects are also subjected to cyclic thermal stresses during operation between start-up and shutdown stages. The fatigue damage of Crofer 22 H under TMF loading without hold time has been discussed in the previous section. However, repeated cycles of start-up, steady operation, and shutdown are expected to take place in practical applications of a pSOFC system. Therefore, it is also needed to investigate whether the fatigue (TMF)-creep interaction would generate any additional damage on the SOFC interconnects in terms of mechanical strength and structural integrity. Therefore, TMF tests with a hold time at 800 °C were also performed in the present study to simulate an operating cycle consisting of start-up, steady operation, and shutdown stages.

Table 4 lists the number of cycles to failure for Crofer 22 H steel subjected to selected TMF loadings with a hold time of 100 h at 800 °C. As shown in Table 4, the number of cycles to failure is similarly increased with a decrease in YSR at 800 °C for the hold-time TMF tests. Similar to the results of TMF tests without hold time, the hold-time TMF life has no dependence on the YSR at 25 °C. As shown in Tables 2 and 4 the hold-time TMF life is much shorter than the non-hold-time one for a given TMF loading combination. The creep damage ratios for the hold-time TMF loadings are calculated in a similar way described in Eq. (6) and given in Table 5. As shown in Tables 3 and 5, the creep damage ratios for the hold-time TMF loadings are significantly larger as compared to the non-hold-time ones with selected YSRs of 0.2 and 0.3 at 800 °C. It indicates that the influence of creep mechanism on the TMF life is increased and can not be neglected for the cases with a hold time of 100 h at 800 °C.

Fig. 5 shows the relationship between the actuator displacement and time during a (0.6, 0.2) TMF loading with a hold time. A similar trend of an increase in specimen deformation with temperature in each cycle is shown in Fig. 5. Again, such a variation of specimen deformation with applied temperature is partially caused by the aforementioned high-temperature softening effect. As shown in Fig. 5, during the hold-time period at 800 °C, the specimen deformation is continuously increased, apparently due to a creep effect. With a greater creep damage ratio for this given hold-time TMF loading, creep mechanism indeed makes certain contributions to the specimen deformation during a loading cycle. Therefore, both high-temperature softening plastic deformation and creep contribute to the damage in TMF loadings with a hold time at 800 °C.

3.3. Thermo-mechanical fatigue life and damage analyses

As shown in Fig. 2, the relation between the non-hold-time TMF life and YSR at 800 °C for all YSRs at 25 °C follows a logarithmic function. The fitted equation and correlation coefficient for all data points shown in Fig. 2 are given as follows:

$$YSR_{800} = -0.111 \ln\left(N_f\right) + 0.688, \quad r^2 = 0.95 \tag{7}$$

where YSR_{800} is the YSR at 800 °C and r is the correlation coefficient for the fitted curve. The high value of correlation coefficient indicates that the non-hold-time TMF life for the Crofer 22 H steel can be predicted through the logarithmic function.

Fig. 6 shows the relationship between the non-hold-time TMF life and applied stress range for various YSRs at 25 °C. As shown in Fig. 6, TMF life is increased with stress range for a given YSR at 25 °C. The variation of TMF life with stress range for such a steel for each given YSR at 25 °C can also be described by a logarithmic function. Note that, for a YSR of 0.5, there are only two points used for curve fitting. The fitted equations and associated correlation coefficients for each YSR at 25 °C in Fig. 6 are given as follows:

$$\text{YSR of 0.6 at 25°C:} \quad \sigma_r = 16.1 \ln\left(N_f\right) + 156, \quad r^2 = 0.98 \tag{8}$$

$$\text{YSR of 0.5 at 25°C:} \quad \sigma_r = 15.2 \ln\left(N_f\right) + 119, \quad r^2 = 1.0 \tag{9}$$

$$\text{YSR of 0.4 at 25°C:} \quad \sigma_r = 12.0 \ln\left(N_f\right) + 82.9, \quad r^2 = 0.99 \tag{10}$$

$$\text{YSR of 0.2 at 25°C:} \quad \sigma_r = 12.9 \ln\left(N_f\right) - 2.90, \quad r^2 = 0.96 \tag{11}$$

where σ_r is the applied stress range in unit of MPa. The non-hold-time TMF life of Crofer 22 H for a given YSR at 25 °C can thus be

Table 4
Number of cycles to failure for Crofer 22 H steel under selected hold-time TMF loadings.

Hold-time TMF loading	Number of cycles to failure
(0.2, 0.3)	0.5
(0.3, 0.3)	0.4
(0.4, 0.2)	4.5
(0.4, 0.3)	0.5
(0.6, 0.2)	2.5
(0.6, 0.3)	0.3

Table 5
Damage ratios of creep, fatigue, and creep–fatigue interaction for Crofer 22 H under selected hold-time TMF loadings.

Hold-time TMF loading	Creep damage ratio	Fatigue damage ratio	Creep-fatigue interaction damage ratio
(0.2, 0.3)	0.20	0.03	0.77
(0.3, 0.3)	0.14	0.03	0.83
(0.4, 0.2)	0.52	0.05	0.43
(0.4, 0.3)	0.22	0.03	0.75
(0.6, 0.2)	0.32	0.05	0.63
(0.6, 0.3)	0.08	0.05	0.87

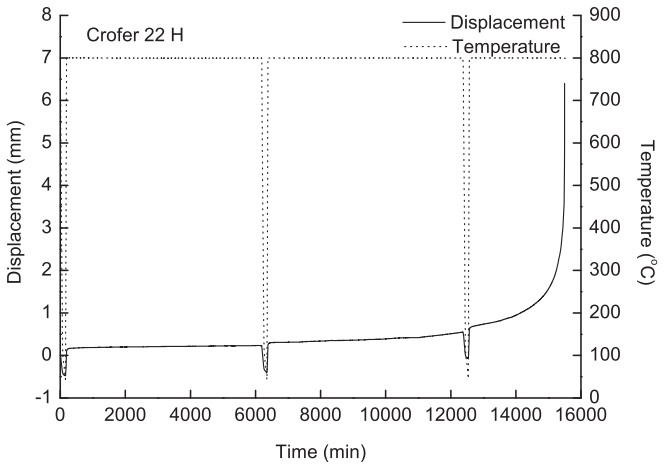

Fig. 5. Typical variation of displacement with time for Crofer 22 H steel under a (0.6, 0.2) TMF loading with a hold time of 100 h.

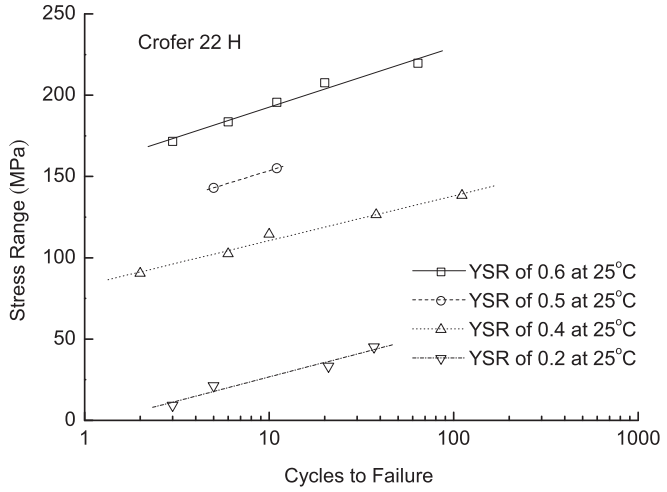

Fig. 6. Relationship between non-hold-time TMF life and applied stress range for Crofer 22 H steel with various YSRs at 25 °C.

estimated through these logarithmic functions once the stress range is known.

As described in Section 2.2, the apparent YSR for each TMF test was determined based on the tensile yield strength under a displacement rate of 2 mm min^{-1}. However, the true displacement rate during the heating step in the given TMF tests is around 0.02 mm min^{-1}, as shown in Figs 3 and 5. It has been reported that high-temperature yield strength is decreased with decreasing strain rate for ferritic and ferritic-martensitic steels [27,28]. In order to further understand the effect of high-temperature softening plastic deformation on the non-hold-time TMF behavior, an additional tensile test under displacement control with a loading rate of 0.02 mm min^{-1} was performed at 800 °C to obtain the corresponding yield strength. The yield strength of Crofer 22 H under a displacement rate of 0.02 mm min^{-1} is determined as 72.9 MPa at 800 °C, while it is 120 MPa for 2 mm min^{-1}. Apparently, the true YSRs at 800 °C in the given TMF tests are much larger than the apparent ones due to such a significant reduction of yield strength for a true, lower loading rate. Table 6 lists the apparent and true YSRs in the given TMF loadings at 800 °C for comparison. As shown in Table 6, each true YSR is significantly larger than the corresponding, apparent one. It means that the cyclic high-temperature softening plastic deformation in the given non-hold-time TMF loadings is more damaging than expected. This might explain why the contribution of cyclic plastic deformation to the damage in the non-hold-time TMF loading is significantly greater than that of creep.

To evaluate the effects of cyclic plastic deformation on the hold-time TMF life, a fatigue damage ratio for the hold-time TMF loadings can be estimated through a linear cumulative damage rule using the non-hold-time TMF life. Calculation of the fatigue damage ratio is given below:

$$D_f = \frac{N_h}{N_n} \tag{12}$$

where D_f is the fatigue damage ratio, N_h is the number of cycles to failure for a given hold-time TMF loading, and N_n is the number of cycles to failure for the corresponding non-hold-time TMF case. Therefore, the fatigue damage ratio for each hold-time case is calculated using the number of cycles to failure in Table 4 divided by the corresponding one of the non-hold-time TMF case (Table 2) with a similar combination of peak/valley loading. As listed in Table 5, the fatigue damage ratio for each hold-time TMF loading is in the range of 0.03–0.05 indicating a very small effect of pure

Table 6
Apparent and true yield strength ratios of TMF loading at 800 °C for Crofer 22 H.

Apparent yield strength ratio at 800 °C	True yield strength ratio at 800 °C
0.2	0.33
0.3	0.49
0.4	0.66
0.5	0.82
0.6	0.99

fatigue mechanism. In addition, a sum of fatigue and creep damage ratios (Table 5) for each given TMF test with a hold time still has a value less than unity. A synergistic action of fatigue and creep apparently generates more damages than would be expected from the algebraic sum of the individual effects of fatigue and creep in the present study. It has been reported that the final fracture of a ferritic steel and alloy under a hold-time TMF loading involves a creep–fatigue interaction mechanism [25,26]. Therefore, it is suggested that a creep–fatigue interaction mechanism is involved in each given hold-time TMF loading in the current study. Damage ratio for such a creep–fatigue interaction effect is estimated by means of a linear cumulative damage rule through the following equation:

$$D_f + D_c + D_{fc} = 1 \tag{13}$$

where D_{fc} is the damage ratio of creep–fatigue interaction for a given hold-time TMF case. Accordingly, the damage ratio of creep–fatigue interaction for each hold-time TMF loading is readily obtained by subtracting from unity a sum of the fatigue and creep damage ratios (Table 5). As shown in Tables 4 and 5, a greater creep–fatigue interaction damage ratio resulted in a shorter hold-time TMF life. As also shown in Tables 4 and 5, the contribution

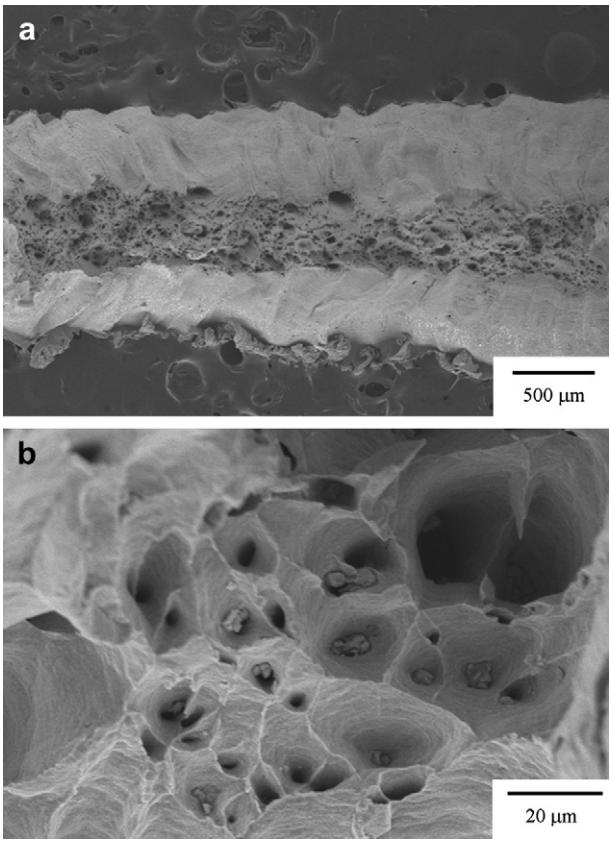

Fig. 7. Fractographs of a Crofer 22 H specimen under a non-hold-time (0.5, 0.4) TMF loading: (a) low magnification; (b) High magnification.

of creep to the damage in a hold-time TMF loading is increased with a decrease in YSR at 800 °C (e.g. from 0.3 to 0.2) and an increase in number of cycles to failure. In addition, the lifetime of a hold-time TMF test is significantly shorter than the expected, pure creep lifetime following the relations in Eqs. (4) and (5) for a similar constant loading during the hold-time period. This is due to a creep–fatigue interaction effect. Therefore, the hold-time TMF life for YSRs of 0.2 and 0.3 at 800 °C varies with extent of influence of creep and creep–fatigue interaction mechanisms. As the hold time for a long-term steady operation of a pSOFC system is generally greater than 100 h and even over 1000 h, it is expected that the influence of creep on the hold-time TMF damage would be more significant for practical applications of the given interconnect steel. Creep properties of such ferritic stainless steels (Crofer 22 H and Crofer 22 APU) for use as an interconnect material in pSOFCs have been fully investigated in previous studies [17,18].

3.4. Microstructural and fractography analyses

SEM micrographs of the fracture surface of a Crofer 22 H specimen after a non-hold-time TMF test with a (0.5, 0.4) loading are shown in Fig. 7. A fractured, cross-sectional area with significant necking is observed in Fig. 7(a). Such a significant reduction of cross-sectional area is attributed to a high-temperature softening effect. As shown in Fig. 7(b), a ductile fracture mode is identified by the dimpled patterns at a high magnification. Most of the non-hold-time TMF fracture surfaces for high YSRs at 800 °C are characterized by such a facture pattern due to their extremely short TMF life (<35 cycles). Fig. 8 shows a fractograph of a Crofer 22 H specimen after a non-hold-time (0.3, 0.3) TMF test. As shown in Fig. 8(a), a stable fatigue crack propagation zone is observed at the right part of the fracture surface, while the left part is the final ductile fracture zone. Striations on the fracture surface, as shown in Fig. 8(b), are the evidence of a fatigue crack propagation mechanism. Such a fatigue cracking pattern becomes more evident as the number of cycles to failure is increased. Therefore, the fracture mode of the non-hold-time TMF behavior is basically controlled by a fatigue mechanism involving cyclic high-temperature softening plastic deformation.

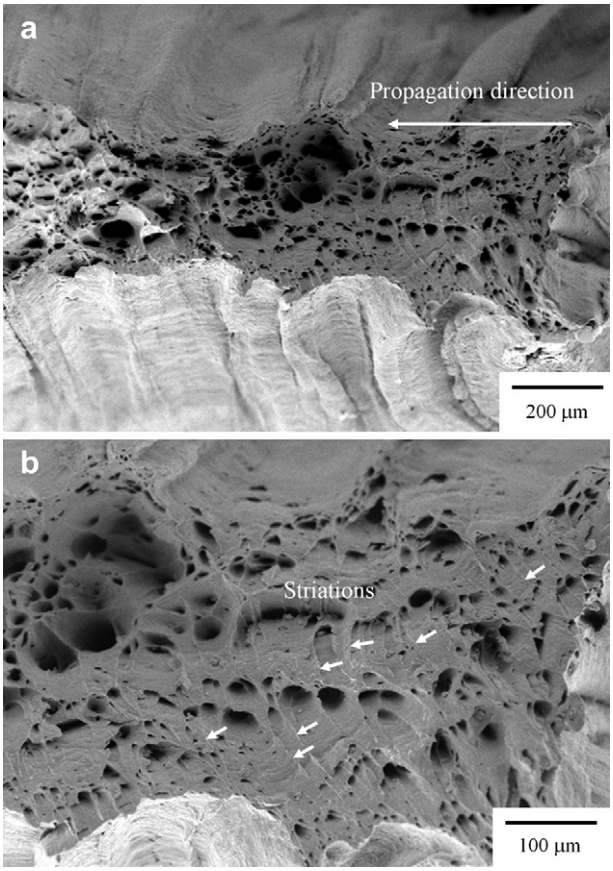

Fig. 8. Fractographs of a Crofer 22 H specimen under a non-hold-time (0.3, 0.3) TMF loading: (a) low magnification; (b) High magnification.

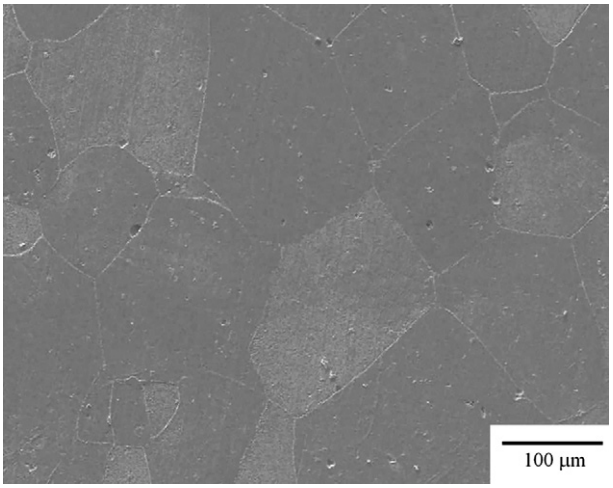

Fig. 9. SEM micrograph of microstructure in the Crofer 22 H specimen before TMF test.

An SEM micrograph of the Crofer 22 H microstructure before TMF test is shown in Fig. 9. Ferritic grain boundaries are observed in Fig. 9 and the average grain size is about 155 μm. There are some precipitates and voids in the micrograph. During metallography specimen preparation, the debonded precipitates left the voids in the microstructure. After a hold-time TMF test, a similar ductile fracture pattern of that in Fig. 7 is also observed, due to the aforementioned high-temperature softening effect. In addition, substantial creep cavities are found in the Crofer 22 H microstructure after a hold-time TMF test. Fig. 10 shows an SEM micrograph of the microstructure after a hold-time TMF test with a (0.6, 0.2) loading. As shown in Fig. 10, coalescence of creep cavities is found in the microstructure, particularly along the grain boundaries. Such a creep damage in the given steel is enlarged at low YSRs at 800 °C. Creep cavities are barely found in the specimens after the non-hold-time TMF tests. This provides evidence that creep–fatigue interaction and creep mechanisms both play a role in determining the fracture mode and life of the hold-time TMF specimens.

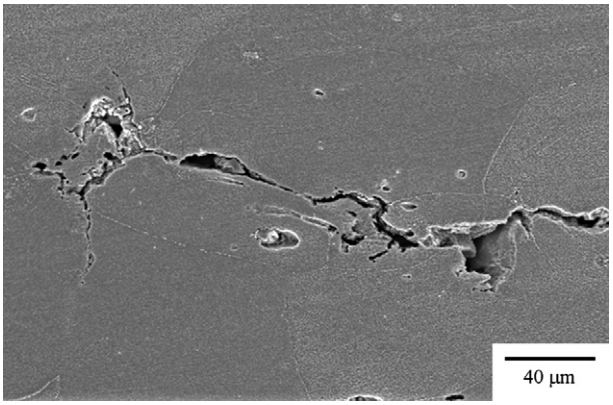

Fig. 10. SEM micrograph of a Crofer 22 H microstructure under a hold-time (0.6, 0.2) TMF loading.

4. Conclusions

1. A fatigue mechanism involving cyclic plastic deformation plays an important role in influencing the non-hold-time TMF life of Crofer 22 H steels. A greater extent of cyclic high-temperature softening plastic deformation results in a smaller number of cycles to failure.
2. The number of cycles to failure for non-hold-time TMF loading is increased with a decrease in applied stress at high temperature. However, for a given applied stress at 800 °C, the non-hold-time TMF life is barely dependent on the applied stress at room temperature. The non-hold-time TMF life is well described by a logarithmic function of applied stress (expressed as yield strength ratio) at 800 °C.
3. A synergy of fatigue and creep in the hold-time TMF loading generates more damages and a much smaller number of cycles to failure than would be expected from the algebraic sum of the individual effects of fatigue and creep.
4. The creep and creep–fatigue interaction are the two controlling effects involved in the hold-time TMF damage of Crofer 22 H steels. The contribution of creep to the damage in a hold-time TMF loading is increased with a decrease in applied stress at 800 °C and an increase in number of cycles to failure.
5. Both ductile, dimpled fracture and fatigue cracking patterns are identified for the Crofer 22 H specimens after a non-hold-time TMF test with a longer TMF life (>35 cycles). The fracture mode of the non-hold-time TMF behavior is basically controlled by cyclic plastic deformation. Coalescence of creep cavities is found along the grain boundaries after a hold-time TMF test.

Acknowledgment

This work was supported by the National Science Council (Taiwan) under Contract No. NSC 99-2221-E-008-012-MY3.

References

[1] H. Yokokawa, N. Sakai, T. Horita, K. Yamaji, Fuel Cells 1 (2001) 117–131.
[2] W.Z. Zhu, S.C. Deevi, Mater. Sci. Eng. A 348 (2003) 227–243.
[3] A. Weber, E. Ivers-Tiffée, J. Power Sources 127 (2004) 273–283.
[4] I. Antepara, I. Villarreal, L.M. Rodriguez-Martinez, N. Lecanda, U. Castro, A. Laresgoiti, J. Power Sources 151 (2005) 103–107.
[5] J.W. Fergus, Mater. Sci. Eng. A 397 (2005) 271–283.
[6] K. Huang, P. Hou, J. Goodenough, Solid State Ionics 129 (2000) 237–250.
[7] C.-K. Lin, T.-T. Chen, Y.-P. Chyou, L.-K. Chiang, J. Power Sources 164 (2007) 238–251.
[8] C.-K. Lin, L.-H. Huang, L.-K. Chiang, Y.-P. Chyou, J. Power Sources 192 (2009) 515–524.
[9] H. Apfel, M. Rzepka, H. Tu, U. Stimming, J. Power Sources 154 (2006) 370–378.
[10] V. Shankar, V. Bauer, R. Sandhya, M.D. Mathew, H.-J. Christ, J. Nucl. Mater. 420 (2012) 23–30.
[11] Y.-P. Chyou, T.-D. Chung, J.-S. Chen, R.-F. Shie, J. Power Sources 139 (2005) 126–140.
[12] H. Kurokawa, K. Kawamura, T. Maruyama, Solid State Ionics 168 (2004) 13–21.
[13] Z. Yang, G.-G. Xia, M.S. Walker, C.-M. Wang, J.W. Stevenson, P. Singh, Int. J. Hydrogen Energy 32 (2007) 3770–3777.
[14] S.J. Geng, J.H. Zhu, Z.G. Lu, Solid State Ionics 177 (2006) 559–568.
[15] P.E. Gannon, C.T. Tripp, A.K. Knospe, C.V. Ramana, M. Deibert, R.J. Smith, V.I. Gorokhovsky, V. Shutthanandan, D. Gelles, Surf. Coat. Technol. 188-189 (2004) 55–61.
[16] S. Fontana, R. Amendola, S. Chevalier, P. Piccardo, G. Caboche, M. Viviani, R. Molins, M. Sennour, J. Power Sources 171 (2007) 652–662.
[17] Y.-T. Chiu, C.-K. Lin, J.-C. Wu, J. Power Sources 196 (2011) 2005–2012.
[18] Y.-T. Chiu, C.-K. Lin, J. Power Sources 198 (2012) 149–157.
[19] J. Froitzheim, G.H. Meier, L. Niewolak, P.J. Ennis, H. Hattendorf, L. Singheiser, W.J. Quadakkers, J. Power Sources 178 (2008) 163–173.
[20] B. Kuhn, C.A. Jimenez, L. Niewolak, T. Hüttel, T. Beck, H. Hattendorf, L. Singheiser, W.J. Quadakkers, Mater. Sci. Eng. A 528 (2011) 5888–5899.
[21] H.-T. Chang, C.-K. Lin, C.-K. Liu, J. Power Sources 189 (2009) 1093–1099.
[22] H.-T. Chang, C.-K. Lin, C.-K. Liu, J. Power Sources 195 (2010) 3159–3165.
[23] H.-T. Chang, C.-K. Lin, C.-K. Liu, S.-H. Wu, J. Power Sources 196 (2011) 3583–3591.
[24] C.-K. Lin, J.-Y. Chen, J.-W. Tian, L.-K. Chiang, S.-H. Wu, J. Power Sources 205 (2012) 307–317.
[25] F. Colombo, E. Mazza, S.R. Holdsworth, R.P. Skelton, Int. J. Fatigue 30 (2008) 241–248.
[26] D.-Q. Shi, J.-L. Liu, X.-G. Yang, H.-Y. Qi, J.-K. Wang, Mater. Sci. Eng. A 528 (2010) 233–238.
[27] P.F. Giroux, F. Dalle, M. Sauzay, J. Malaplate, B. Fournier, A.F. Gourgues-Lorenzon, Mater. Sci. Eng. A 527 (2010) 3984–3993.
[28] M.A. Sokolov, D.T. Hoelzer, R.E. Stoller, D.A. McClintock, J. Nucl. Mater. 367-370 (2007) 213–216.